Biosensors and Bioelectronics 25 (2009) 428–434

Contents lists available at ScienceDirect

Biosensors and Bioelectronics

journal homepage: www.elsevier.com/locate/bios

Conductive architecture of Fe_2O_3 microspheres/self-doped polyaniline nanofibers on carbon ionic liquid electrode for impedance sensing of DNA hybridization

Wei Zhang, Tao Yang, Xiao Li, Debao Wang, Kui Jiao*

Key Laboratory of Eco-chemical Engineering (Ministry of Education), College of Chemistry and Molecular Engineering, Qingdao University of Science and Technology, Qingdao 266042, China

ARTICLE INFO

Article history:
Received 8 June 2009
Received in revised form 24 July 2009
Accepted 28 July 2009
Available online 4 August 2009

Keywords:
Fe_2O_3 microspheres
SPAN nanofibers
Carbon ionic liquid electrode
DNA electrochemical biosensor
PEPCase gene

ABSTRACT

A novel architecture was designed by combining the strong adsorption ability of Fe_2O_3 microspheres to the DNA probes and excellent conductivity of self-doped polyaniline (SPAN) nanofibers (copolymer of aniline and *m*-aminobenzenesulfonic acid) on carbon ionic liquid electrode (CILE) for electrochemical impedance sensing of the immobilization and hybridization of DNA. The formed conductive Fe_2O_3/SPAN membrane on the CILE was characterized by cyclic voltammetry (CV) and electrochemical impedance spectroscopy (EIS) using $[Fe(CN)_6]^{3-/4-}$ as the indicator. The immobilization of the probe DNA on the surface of electrode and the sensitivity of DNA hybridization recognition were dramatically enhanced due to the unique synergistic effect of Fe_2O_3 microspheres, SPAN nanofibers and ionic liquid. The DNA hybridization events were monitored with a label-free EIS strategy. Under optimal conditions, the dynamic range of this DNA biosensor for detecting the sequence-specific DNA of phosphoenolpyruvate carboxylase (PEPCase) gene from transgenically modified rape was from 1.0×10^{-13} to 1.0×10^{-7} mol/L, and the detection limit was 2.1×10^{-14} mol/L. This work suggested a simple strategy to prepare a conductive interface for electrochemical detection of DNA hybridization and opened a way for the application of Fe_2O_3 in DNA electrochemical biosensing.

1. Introduction

Nucleic acid hybridization has become one of the most important techniques in molecular biology for the detection and analysis of specific DNA sequences. Determination of nucleic acid sequences plays an increasingly significant role in many fields, ranging from clinical diagnosis, forensic analysis and drug research to food safety monitoring (Y.L. Zhang et al., 2009). A variety of approaches have been developed for the detection of DNA hybridization, including fluorescent, electrochemical, piezoelectric, and acoustic techniques (Teles and Fonseca, 2008). Among these techniques, electrochemical methods have attracted significant attention for their simplicity, reliability, selectivity, and sensitivity as well as compatibility with microfabrication technology. Thus, in recent years, there has been considerable interest in developing DNA electrochemical biosensors for the rapid and inexpensive diagnosis of genetic diseases and other biological analysis (Prabhakar et al., 2008; Chen et al., 2008; Gorodetsky et al., 2008; Li et al., 2008; Yang et al., 2009). Generally, the main target for the fabrication of DNA biosensors is to prepare well-defined DNA recognition interface for effective immobilization of probe ssDNA onto transducer surface through suitable matrix and immobilization method.

Due to their special attributes, magnetic particles have been used in drug delivery, hyperthermia treatment, cell separation, and immunoassay (Sonti and Bose, 1995; Cheng et al., 2005; Ao et al., 2006). Recently, magnetic particles as special biomolecular immobilizing carriers are becoming the focus of research, since magnetic behavior of these bioconjugates is likely to improve delivery and recovery of biomolecules for desired biosensing applications (S.F. Wang et al., 2008; Zhuo et al., 2009; Tang et al., 2008; Cheng et al., 2009). For instance, Wang et al. developed a novel tyrosinase biosensor based on Fe_3O_4–chitosan nanocomposite for the detection of phenolic compounds (S.F. Wang et al., 2008). Zhuo et al. reported an electrochemical immunosensor of high selectivity and good reproducibility with the employment of bienzyme functionalized three-layer composite magnetic particles (Zhuo et al., 2009). In this context, Fe_2O_3, as one of the most important magnetic metal oxides, may act as a promising immobilization carrier for biosensing owing to its unusual properties including high conductivity, low toxicity, and easy preparation process (Qu et al., 2007).

The choice of a suitable supporting material is an important factor that may affect the performance of supported analytes owing to the support–analyte interactions and surface reactivity. Room temperature ionic liquid (RTIL), comprising of organic cations and various anions, represents a new kind of nonaqueous but polar

* Corresponding author. Tel.: +86 532 84022665; fax: +86 532 84023927.
E-mail address: kjiao@qust.edu.cn (K. Jiao).

0956-5663/$ – see front matter © 2009 Elsevier B.V. All rights reserved.
doi:10.1016/j.bios.2009.07.032

solvents, which possesses many good characteristics, such as negligible vapor pressure, noninflammability, high ionic conductivity, fine thermal stability and wide electrochemical window (Welton, 1999). Recently, carbon ionic liquid electrode (CILE) has been proposed and widely applied in the electrochemical community (Maleki et al., 2008; Shangguan et al., 2008; Musameh et al., 2008; Sun et al., 2007, 2008; Franzoi et al., 2009). Using ionic liquid as a very efficient pasting binder in place of nonconductive organic binders in carbon paste electrode (CPE) allows us to construct a new generation of carbon composite electrode with advantages over traditional CPE's such as excellent conductivity, renewable surface, fast electron-transfer rate and high sensitivity for detection. For example, Maleki et al. explored a palladium nanoparticle decorated CILE for highly efficient electrocatalytic oxidation and determination of hydrazine (Maleki et al., 2008). Shangguan et al. studied the direct electrochemistry of glucose oxidase based on its direct immobilization on CILE (Shangguan et al., 2008). However, to the best of our knowledge, the application of CILE as the biosensing construction platform for detection of DNA hybridization has rarely been reported.

The aim of this work is to develop a simple and effective conduction route, which provides a well-defined recognition surface for hybridization. In this study, a membrane composed of Fe_2O_3 microspheres and self-doped polyaniline (SPAN) nanofibers was constructed on CILE as the platform for label-free detection of DNA hybridization. In detail, SPAN nanofibers were firstly coated on the surface of a CILE to form a negatively charged nanostructured monolayer. Then the positively charged Fe_2O_3 microspheres (isoelectric point ~7.0) were adsorbed on the SPAN/CILE surface by electrostatic attraction with the SO_3^{2-} of SPAN nanofibers (Radeva and Petkanchin, 1997; Gao et al., 2007). The obtained Fe_2O_3/SPAN/CILE integrated the strong adsorption ability of Fe_2O_3 microspheres to the DNA probes with the large surface area and excellent electron-transfer ability of SPAN nanofibers, and the high conductivity of CILE. The synergistic effect of this matrix could greatly enhance the loading of DNA probes, the electron transfer of $[Fe(CN)_6]^{3-/4-}$ (the redox indicator for EIS) and hence markedly improve the sensitivity of target DNA detection. The fabricated biosensor was applied to label-free detection of the DNA specific sequences of phosphoenolpyruvate carboxylase (PEPCase) gene from transgenically modified rape with satisfactory results.

2. Experimental

2.1. Apparatus

All the electrochemical measurements were performed on a CHI 660C electrochemical workstation (Shanghai CH Instrument Company, China). A conventional three-electrode system was used with a modified CILE as working electrode, a saturated calomel electrode (SCE) as reference electrode and a platinum wire as auxiliary electrode. The pH values of all solutions were measured by a model pHS-25 digital acidimeter (Shanghai Leici Factory, China). Scanning electron microscopy (SEM) was carried out using a JSM-6700F machine (JEOL, Tokyo, Japan).

2.2. Chemicals

Ionic liquid 1-butyl-3-methylimidazolium hexafluorophosphate ($BMIMPF_6$, Hangzhou Kemer Chemical Limited Company, China), graphite powder (average particle size 30 μm, Shanghai Colloid Chemical Plant, China), potassium ferricyanide ($K_3[Fe(CN)_6]$, Shanghai No. 1 Reagent Factory, China) and potassium ferrocyanide ($K_4[Fe(CN)_6]$, Shanghai Heng Da Chemical Limited Company, China) were used as received. SPAN nanofibers were prepared according to the reference (C.Q. Zhang et al., 2009) and dispersed in ultrapure water to 2.0 mg/mL. Fe_2O_3 microspheres were synthesized as reported previously (D.B. Wang et al., 2008) and dispersed in Britton-Robinson (B-R) buffer (pH 3.0) to 2.0 mg/mL. All the chemicals were of analytical grade and ultrapure water was used in all the experiments.

Materials for detection of PEPCase gene sequences: The 20-base oligonucleotides probe (ssDNA), its complementary DNA sequence (cDNA, target DNA, namely a 20-base fragment of PEPCase gene sequence, which was selected according to the transgenic sequence of phosphoenolpyruvate carboxylase gene in transgenically modified rape), single-base mismatched DNA sequence, double-base mismatched DNA sequence and noncomplementary DNA sequence (ncDNA) were synthesized by Beijing SBS Gene Technology Limited Company. Their base sequences are listed below:

probe DNA (ssDNA): 5′-CAG CAC CTA GGC ATA GGT TC-3′;
target DNA (cDNA): 5′-GAA CCT ATG CCT AGG TGC TG-3′;
single-base mismatched DNA: 5′-GAA CCT ATG CCT AGG TGG TG-3′;
double-base mismatched DNA: 5′-GAA CCT CTG CCT AGG TGG TG-3′;
ncDNA: 5′-TGC GAT AAA GGA AAG GCT AT-3′.

All oligonucleotides stock solutions of 20-base oligomers (1.0×10^{-7} mol/L) were prepared with Tris–HCl buffer (5.0 mmol/L Tris–HCl, 50.0 mmol/L NaCl, pH 7.0), and stored at 4 °C. More diluted solutions were obtained via diluting aliquot of the stock solution with ultrapure water prior to use. The hybridization solution was diluted with 2× SSC (pH 7.5), which consisted of 0.30 mol/L NaCl and 0.03 mol/L sodium citrate tribasic dihydrate ($C_6H_5Na_3O_7 \cdot 2H_2O$).

2.3. Preparation of CILE and Fe_2O_3/SPAN/CILE

The traditional CPE was prepared by hand-mixing of graphite powder with solid paraffin at a ratio of 3/1 (w/w) in an agate mortar. The homogeneous paste was packed firmly into one end of a glass tube with the diameter of 4 mm. The electrical contact was provided by inserting a copper wire to the paste in the inner hole of the tube. The CILE was prepared by the procedure similar to that of traditional CPE only with changes by mixing ionic liquid $BMIMPF_6$ with graphite powder at a ratio of 1/4 (w/w) in a mortar.

Prior to modification, the surface of the electrode was smoothed with a weighting paper. 10 μL of 2.0 mg/mL SPAN nanofibers suspension was spread uniformly onto the surface of the CILE and air-dried naturally to obtain the SPAN/CILE. Then 10 μL of 2.0 mg/mL Fe_2O_3 microspheres suspension was placed on the SPAN/CILE and allowed to dry at room temperature, thus a uniform membrane coated electrode (Fe_2O_3/SPAN/CILE) was obtained.

2.4. Immobilization and hybridization of DNA

Immobilization of ssDNA probes was performed by immersing the Fe_2O_3/SPAN/CILE into 2.0 mL Tris–HCl buffer solution (pH 7.0) containing 1.0×10^{-7} mol/L ssDNA probes with a constant potential at 0.7 V for 600 s, followed by washing the electrode with 0.5% sodium dodecylsulfate (SDS) solution and then rinsing it with ultrapure water to remove the unimmobilized ssDNA, and this probe-captured electrode was denoted as ssDNA/Fe_2O_3/SPAN/CILE.

The ssDNA/Fe_2O_3/SPAN/CILE was immersed into a hybridization solution (2× SSC buffer, pH 7.5) containing the target DNA and hybridized at 0.4 V for 500 s, followed by washing the electrode with 0.5% SDS solution to remove the unhybridized

DNA, and this hybridization modified electrode was denoted as dsDNA/Fe_2O_3/SPAN/CILE. The hybridizations of probe ssDNA with single-base mismatched DNA, double-base mismatched DNA and ncDNA were carried out through similar procedure.

2.5. Electrochemical measurements

Cyclic voltammetric (CV) and electrochemical impedance spectroscopic (EIS) measurements of 1.0 mmol/L $K_3Fe(CN)_6$ and 1.0 mmol/L $K_4Fe(CN)_6$ were performed with 0.1 mol/L KCl as the supporting electrolyte. The CV scan rate was 100 mV/s. The AC voltage amplitude was 5 mV and the voltage frequencies ranged from 10 kHz to 0.01 Hz. The applied potential was 0.172 V.

The differential pulse voltammetric (DPV) cathodic signals of the accumulated methylene blue (MB) were obtained in B-R buffer (pH 6.0) containing 1.5×10^{-5} mol/L MB. DPV parameters: pulse amplitude 50 mV, pulse width 60 ms, pulse period 0.2 s.

3. Results and discussion

3.1. SEM characterization of SPAN nanofibers and Fe_2O_3 microspheres

The typical SEM image of the prepared SPAN nanofibers is presented in Fig. 1A. It is found that large quantities of well-defined SPAN nanofibers are obtained and they are interconnected together to form netlike nanostructures. The typical length of all the SPAN nanofibers is about several micrometers and their diameters are in the range of 60–80 nm.

Fig. 1B and C display the SEM images of the synthesized Fe_2O_3. The low-magnification SEM image shown in Fig. 1B indicates that the products consist of large amount of monodisperse microparticles, and these microparticles are egglike in shape and uniform in size. The diameter of the Fe_2O_3 microspheres is mainly centered at 500 nm. The high-magnification SEM image in Fig. 1C reveals the surface configuration of the microspheres. It is evident that the surface of the egglike microspheres is not smooth but rough, implying that these microspheres may be composed of smaller subunits.

3.2. Cyclic voltammetric behaviors of the modified electrodes

CV can provide useful information on the barrier changes of the electrode surface during the fabrication process. Therefore, the CV of 1.0 mmol/L $[Fe(CN)_6]^{3-/4-}$ was chosen as a marker to investigate the changes of the electrode behavior before and after each assembly step. As shown in Fig. 2A, a couple of well-defined redox peaks could be observed at the bare CILE (a). After the electrode was coated with SPAN nanofibers, as illustrated in curve b, the current response increased obviously ascribed to the good electron-transfer ability and large electroactive surface area of SPAN nanofibers. The information of the Fe_2O_3/SPAN/CILE was shown in curve c, and there was a further increase of the current response due to the good electrical conductivity of Fe_2O_3 microspheres. For comparison, the current response at the Fe_2O_3/CILE was observed in curve d, which was much lower than that at the Fe_2O_3/SPAN/CILE (c), indicating the synergistic amplification effect of SPAN nanofibers and Fe_2O_3 microspheres on enhancing the current response was outstanding. The current response at the ssDNA/Fe_2O_3/SPAN/CILE (e) decreased dramatically as compared with that at the Fe_2O_3/SPAN/CILE (c), demonstrating that ssDNA probes had been immobilized on the surface of the Fe_2O_3/SPAN membrane. The negatively charged phosphate skeletons of ssDNA immobilized on the membrane had a repulsive force to $[Fe(CN)_6]^{3-/4-}$ anion, and therefore the current response of $[Fe(CN)_6]^{3-/4-}$ at the ssDNA/Fe_2O_3/SPAN/CILE decreased significantly.

As shown in Fig. 2B, the current response of $[Fe(CN)_6]^{3-/4-}$ at the CILE (b) was greater than that at the traditional CPE (a), which

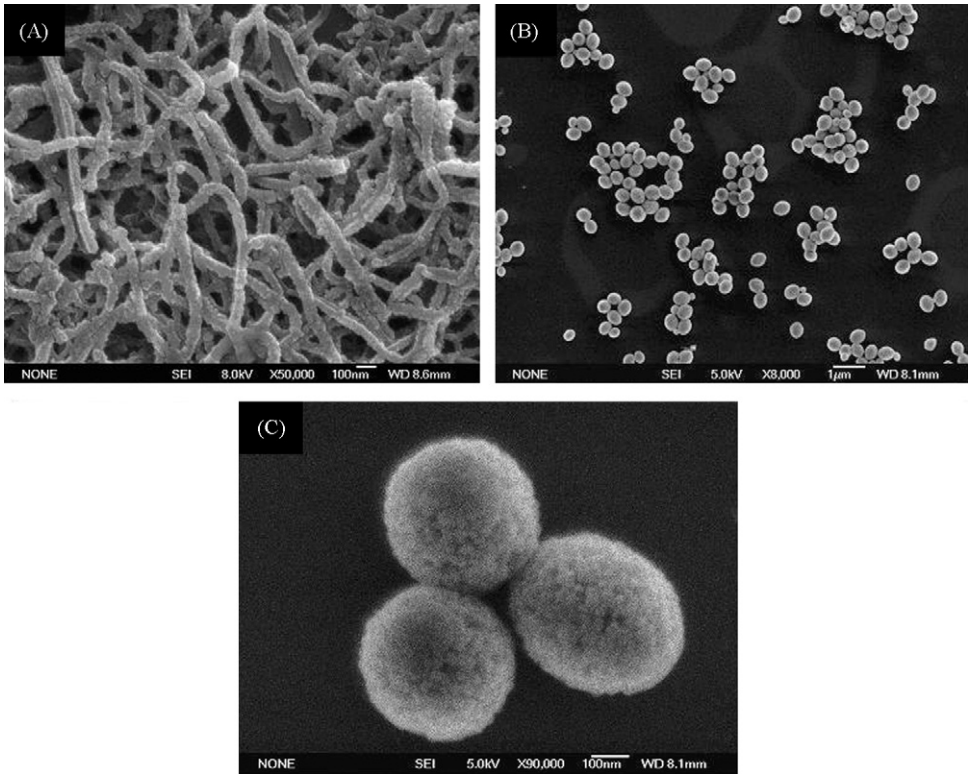

Fig. 1. (A) SEM image of SPAN nanofibers, (B) low-magnification and (C) high-magnification SEM images of Fe_2O_3 microspheres.

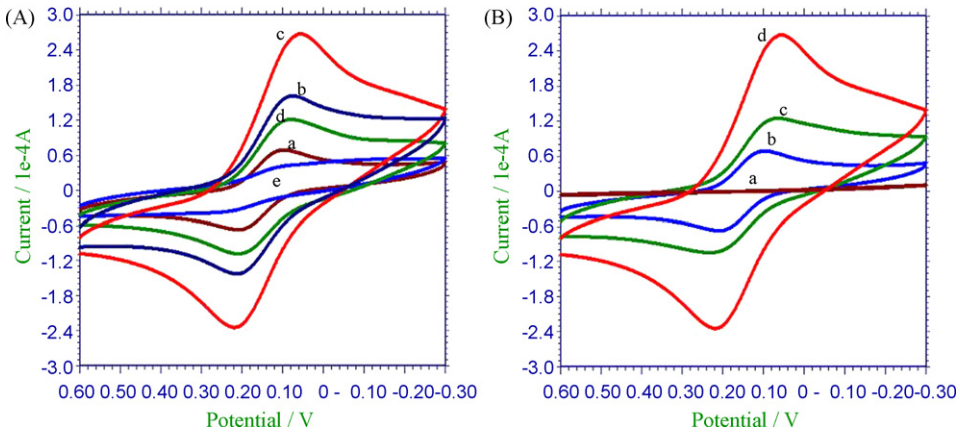

Fig. 2. (A) Cyclic voltammograms of 1.0 mmol/L $[Fe(CN)_6]^{3-/4-}$ recorded at (a) bare CILE, (b) SPAN/CILE, (c) Fe_2O_3/SPAN/CILE, (d) Fe_2O_3/CILE and (e) ssDNA/Fe_2O_3/SPAN/CILE. (B) Cyclic voltammograms of 1.0 mmol/L $[Fe(CN)_6]^{3-/4-}$ recorded at (a) bare CPE, (b) bare CILE, (c) Fe_2O_3/SPAN/CPE and (d) Fe_2O_3/SPAN/CILE.

indicated that the presence of ionic liquid $BMIMPF_6$ with high ionic conductivity in the carbon paste could greatly enhance the conductivity of the electrode. Furthermore, the current response at the Fe_2O_3/SPAN/CILE (d) was also much larger than that at the Fe_2O_3/SPAN/CPE (c). Above experimental results exhibited the superiority of CILE to traditional CPE in terms of improving sensitivity and the potential of CILE as a new generation of biosensing construction platform.

The electroactive surface areas of the electrodes were estimated according to the slope of i_{pa} versus $\nu^{1/2}$ plot, based on the Randles-Sevčik equation (Xiao et al., 2008): $i_{pa} = 2.69 \times 10^5 AD^{1/2} n^{3/2} \nu^{1/2} C$, where i_{pa} refers to the anodic peak current, n the electron-transfer number, A the surface area of the electrode, D the diffusion coefficient, C the concentration of $[Fe(CN)_6]^{3-/4-}$ and ν the scan rate. For 1.0 mmol/L $[Fe(CN)_6]^{3-/4-}$, $n = 1$ and $D = 6.70 \times 10^{-6}$ cm^2/s, then from the slope of the i_{pa}–$\nu^{1/2}$ relation, the active surface areas (average of three measurements) of the bare CILE, SPAN/CILE, Fe_2O_3/CILE and Fe_2O_3/SPAN/CILE can be calculated to be 0.65, 1.29, 1.08 and 2.15 cm^2, respectively. Herein, the synergistic effect of SPAN nanofibers and Fe_2O_3 microspheres on enhancing the electroactive surface area was remarkable.

3.3. Electrochemical impedance characterization of the modifying process

EIS with $[Fe(CN)_6]^{3-/4-}$ as the indicator has been extensively used as an effective tool for electrochemical detection of DNA hybridization (Park et al., 2008; Yang et al., 2009; Kukol et al., 2008). Fig. 3 showed Nyquist plots of impedance for the stepwise electrode modification process. The impedance spectra include a semicircle portion at higher frequencies relating to the electron-transfer-limited process and a linear part at lower frequencies corresponding to diffusion. The increase in the diameter of the semicircle reflects the increase in the interfacial electron-transfer resistance (R_{et}). For the bare CILE (a), the value of R_{et} was 527 Ω. After the modification of SPAN nanofibers, the R_{et} value decreased to 356 Ω (b), indicating that the SPAN nanofibers formed high electron conduction pathways between the electrode and electrolyte, and improved the diffusion of $[Fe(CN)_6]^{3-/4-}$ toward the electrode surface. After Fe_2O_3 microspheres were assembled on the SPAN/CILE, a further decrease of R_{et} (262 Ω) was observed (c), and this could be ascribed to the fine conductivity of Fe_2O_3 microspheres. The R_{et} value increased to 738 Ω (d) after ssDNA probes were immobilized on the Fe_2O_3/SPAN membrane, which could be attributed to the electrostatic repulsion between the negatively charged ssDNA probe and $[Fe(CN)_6]^{3-/4-}$ anion. After the ssDNA probes immobilized on the electrode surface were hybridized with the complementary target DNA (cDNA), the R_{et} value increased dramatically to 3210 Ω (e), indicating that the presence of the formed dsDNA on the electrode. After hybridization, the negative charges on the electrode surface increased remarkably and the surface membrane became thicker, which might raise the R_{et} value. In conclusion, from the changes of the R_{et} value, the immobilization and hybridization of DNA on this Fe_2O_3/SPAN/CILE platform could be understood clearly.

As shown in Fig. S1 (see Supplementary material), the R_{et} value was estimated to 580 Ω (a) after ssDNA probes were immobilized on the Fe_2O_3/SPAN/CPE. When the probe ssDNA was hybridized with its complementary target DNA (cDNA), the R_{et} value increased to 1270 Ω (b). The ratio of R_{et} values between dsDNA/Fe_2O_3/SPAN/CPE and ssDNA/Fe_2O_3/SPAN/CPE was calculated to be 2.2, which was lower than that (4.3) between dsDNA/Fe_2O_3/SPAN/CILE and ssDNA/Fe_2O_3/SPAN/CILE, indicating the superiority of CILE to traditional CPE in terms of improving sensitivity of DNA hybridization detection. As shown in Fig. S2 (see Supplementary material), the R_{et} value was estimated to 1450 Ω (a) after ssDNA probes were immobilized on the Fe_2O_3/CILE. When the probe ssDNA was hybridized with its complementary target DNA (cDNA), the R_{et} value increased to 3910 Ω (b). The ratio of R_{et} values between dsDNA/Fe_2O_3/CILE and ssDNA/Fe_2O_3/CILE was calculated to be 2.7, which was also lower than that (4.3) between dsDNA/Fe_2O_3/SPAN/CILE and ssDNA/Fe_2O_3/SPAN/CILE,

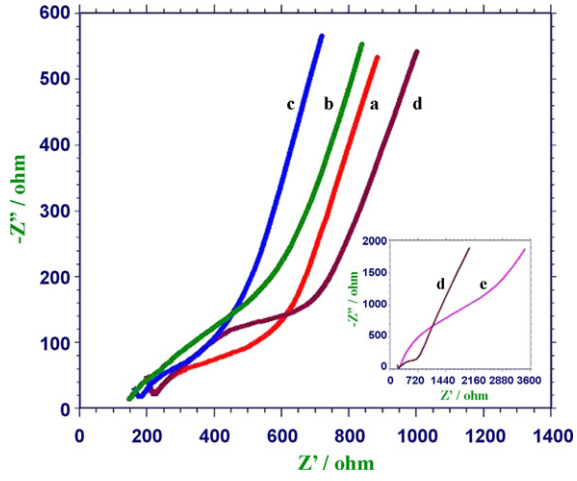

Fig. 3. Nyquist diagrams of 1.0 mmol/L $[Fe(CN)_6]^{3-/4-}$ recorded at (a) bare CILE, (b) SPAN/CILE, (c) Fe_2O_3/SPAN/CILE, (d) ssDNA/Fe_2O_3/SPAN/CILE and (e) dsDNA/Fe_2O_3/SPAN/CILE.

demonstrating that the sensitivity of DNA hybridization detection had been improved when using SPAN nanofibers.

3.4. Differential pulse voltammetry of MB for DNA immobilization and hybridization

MB can be bound specifically to the guanine (G) bases in DNA molecules, and it has been widely used as an electroactive indicator for electrochemical detection of DNA hybridization (Prabhakar et al., 2008; Chen et al., 2008; Zhang et al., 2008a). Fig. S3 (see Supplementary material) displayed the hybridization detection of DNA by using DPV with MB as the indicator. The curve a was the DPV response of MB at the ssDNA/Fe_2O_3/SPAN/CILE. After hybridization of probe ssDNA with the target DNA, the DPV signal of MB decreased remarkably (b), demonstrating that the presence of the formed dsDNA on the electrode. The G bases were embedded in the double helix configuration of the formed dsDNA on the electrode, which prevented MB from accessing the electrode. These phenomena further proved that the Fe_2O_3/SPAN/CILE could be a fine platform for the immobilization and hybridization of DNA.

3.5. Optimization of experimental conditions

The optimal ratio of graphite powder with ionic liquid $BMIMPF_6$ was investigated with the ratio as 6/1, 5/1, 4/1, 3/1 and 2/1 (w/w), respectively, which showed obvious influence on the stability and sensitivity of the CILE. When the amount of $BMIMPF_6$ was too lower, the graphite powder could not be bound together. When the amount of $BMIMPF_6$ was too higher, the background current increased remarkably and the current response of $[Fe(CN)_6]^{3-/4-}$ tended to unstable, which may be due to the partial dissolution of ionic liquid from the electrode surface. Finally, a ratio of 4/1 was selected for the construction of the CILE. As indicated in reference (Maleki et al., 2006), the imidazolium-based ionic liquid showed a strong 'π–π' interaction with graphite powder, which improved the stability of the ionic liquid modified carbon paste.

In the process of electrode modification, the immobilization of the ssDNA probes on the Fe_2O_3/SPAN/CILE was a crucial step. The immobilization potential and time of the probe DNA directly affected its immobilization amount on the Fe_2O_3/SPAN membrane. The probe DNA was immobilized at different potentials, such as 0.4, 0.5, 0.6, 0.7, 0.8 and 0.9 V, and the Nyquist diagrams at the electrode after every immobilization of the probe DNA were respectively recorded. The results showed that the R_{et} value at the probe-modified electrode increased with the positive shift of the potential from 0.4 to 0.7 V, and then reached a constant level beyond 0.7 V. Therefore, 0.7 V was selected for the immobilization of probe DNA in our experiments. The probe DNA was immobilized at 0.7 V for different time from 100 to 900 s, and the results indicated that the R_{et} value increased with the increase of the time from 100 to 600 s. With further increase of the immobilization time, the R_{et} value reached a constant level. An optimal immobilization time of 600 s was used in our experiments.

The hybridization potential and time had important effect on the hybridization reaction. The probe ssDNA/Fe_2O_3/SPAN/CILE was hybridized by immersing it into a hybridization solution containing 1.0×10^{-7} mol/L target DNA at different potentials, such as 0.2, 0.3, 0.4, 0.5 and 0.6 V, for different times (100–700 s), and the Nyquist diagrams at the electrode before and after hybridization of the probe DNA were respectively recorded. The R_{et} difference value after and before hybridization of the probe DNA (ΔR_{et}) was evaluated. The larger the ΔR_{et} value, the better the hybridization. The largest ΔR_{et} value was obtained when the hybridization was conducted at 0.4 V for 500 s. Thus, the optimal hybridization potential was selected as 0.4 V and the optimal hybridization time as 500 s.

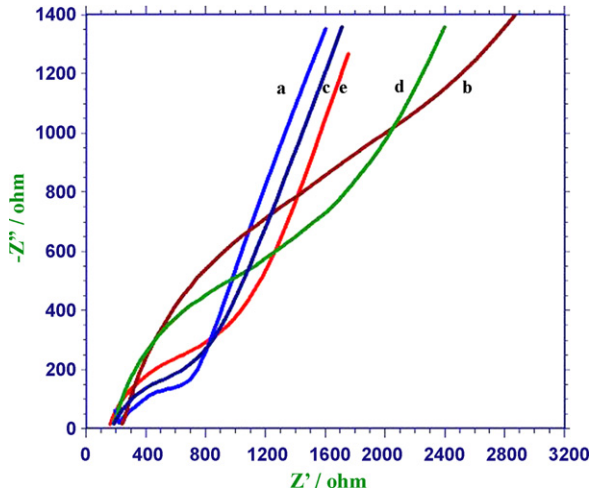

Fig. 4. Nyquist diagrams of 1.0 mmol/L $[Fe(CN)_6]^{3-/4-}$ recorded at (a) ssDNA/Fe_2O_3/SPAN/CILE, (b) dsDNA/Fe_2O_3/SPAN/CILE (hybridization with cDNA), (c) the electrode hybridized with ncDNA, (d) the electrode hybridized with single-base mismatched DNA and (e) the electrode hybridized with double-base mismatched DNA.

3.6. Analytical performance of the DNA biosensor

The selectivity of this DNA biosensor was investigated by using the DNA probe to hybridize with different DNA sequences related to PEPCase gene in transgenically modified rape. After hybridization of the DNA probe, the changes of the Nyquist diagram of 1.0 mmol/L $[Fe(CN)_6]^{3-/4-}$ in 0.1 mol/L KCl were shown in Fig. 4. The curve a was the Nyquist diagram at the probe ssDNA/Fe_2O_3/SPAN/CILE. After hybridization of the DNA probe with the cDNA, the change of the Nyquist diagram was shown in curve b. The R_{et} value increased obviously, suggesting that hybrids (dsDNA) were formed at the electrode. The increase of the R_{et} value was negligible after the DNA probe was hybridized with the ncDNA (c), indicating that the hybridization reaction was not achieved. After the DNA probe was hybridized with the single-base mismatched DNA sequence (d) or double-base mismatched DNA sequence (e), the increase of the R_{et} value was much smaller than that obtained from the hybridization with the cDNA (b). And the single-base mismatched and double-base mismatched DNA sequence could also be recognized via comparing the increase of the R_{et} value. The results demonstrated that this DNA biosensor displayed very high selectivity for the hybridization detection.

The stability of the probe ssDNA/Fe_2O_3/SPAN/CILE was examined by repetitive scanning in 1.0 mmol/L $[Fe(CN)_6]^{3-/4-}$ solution. 97.2% of the initial R_{et} response remained after continuous scanning for 50 cycles. The ssDNA/Fe_2O_3/SPAN/CILE could be stored at 4 °C for about 2 weeks and the decrease of the R_{et} response was got as 3.75%. The results demonstrated that the prepared DNA biosensor had good stability and could be applied for further quantitative analysis. Six parallel-made DNA biosensors were used to detect 1.0×10^{-10} mol/L target DNA and a relative standard deviation (R.S.D.) of 3.58% ($n = 6$) was estimated, showing the high reproducibility of this DNA biosensor.

The regeneration ability of this impedance-based DNA biosensor was also evaluated. The dsDNA on the hybridized electrode was hot denatured by immersing the electrode into boiling water for 10 min, and then cooled down rapidly with an ice salt bath, followed by rinsing the electrode with ultrapure water. The Nyquist diagrams of $[Fe(CN)_6]^{3-/4-}$ at the regenerated probe-modified electrode and its hybridized electrode were recorded. The results indicated that the two R_{et} values at the two electrodes and their ΔR_{et} value were, respectively, almost the same as those obtained in the first experiment. Repetitive experiments showed that the

Table 1
Comparison of the proposed biosensor with other metal oxide-based electrochemical DNA hybridization biosensors.

Electrodes	Methods	Detection range (mol/L)	Detection limit (mol/L)	References
ZrO_2/Au	DPV (MB)	2.25×10^{-10} to 2.25×10^{-8}	1.0×10^{-10}	Zhu et al. (2004)
CeO_2/CHIT/GCE	DPV (MB)	1.59×10^{-11} to 1.16×10^{-7}	1.0×10^{-11}	Feng et al. (2006)
MWNTs/ZrO_2/CHIT/GCE	DPV (daunomycin)	1.49×10^{-10} to 9.32×10^{-8}	7.5×10^{-11}	Y.H. Yang et al. (2007)
ZrO_2/SWNTs/PDC/GCE	EIS	1.0×10^{-11} to 1.0×10^{-6}	1.38×10^{-12}	J. Yang et al. (2007)
ZrO_2/NG/GCE	DPV (MB)	1.0×10^{-10} to 1.0×10^{-6}	3.1×10^{-11}	Zhang et al. (2008b)
ZnO/MWNTs/CHIT/GCE	DPV (MB)	1.0×10^{-11} to 1.0×10^{-6}	2.8×10^{-12}	Zhang et al. (2008a)
CeO_2-SWNTs-$BMIMPF_6$/GCE	EIS	1.0×10^{-12} to 1.0×10^{-7}	2.3×10^{-13}	W. Zhang et al. (2009)
Fe_2O_3/SPAN/CILE	EIS	1.0×10^{-13} to 1.0×10^{-7}	2.1×10^{-14}	This work

DNA biosensor could be reproduced for five times without losing its sensitivity, exhibiting the fine regeneration ability of this DNA biosensor.

3.7. Quantitative analysis of PEPCase gene target sequence

The difference between the R_{et} values (namely ΔR_{et}) of 1.0 mmol/L $[Fe(CN)_6]^{3-/4-}$ containing 0.1 mol/L KCl at the probe ssDNA/Fe_2O_3/SPAN/CILE and that at the hybridization modified electrode (dsDNA/Fe_2O_3/SPAN/CILE) was used to be the measurement signal for quantitative analysis of the PEPCase gene target sequence. The concentration of the PEPCase gene target sequence in the hybridization solution was changed from 1.0×10^{-7} to 1.0×10^{-13} mol/L, and the results were shown in Fig. 5. The ΔR_{et} value between before and after hybridization was linear with the logarithm of the PEPCase gene target sequence concentrations in the range of 1.0×10^{-13} to 1.0×10^{-7} mol/L with a correlation coefficient (R) of 0.9960. The regression equation was $\Delta R_{et} = 3.162 \lg C + 30.737$ (C, mol/L; ΔR_{et}, Ω), and a detection limit of 2.1×10^{-14} mol/L could be estimated using 3σ (where σ was the R.S.D. of the blank solution, $n = 11$). The results demonstrated that the sensitivity of this impedance-based DNA biosensor was good enough for the PEPCase gene sequence detection.

The comparison of the proposed biosensor with other electrochemical biosensors for DNA hybridization detection based on metal oxide was listed in Table 1. From the results it can be seen that this DNA hybridization biosensor displayed a much lower detection limit and wider detection range for the target DNA assay.

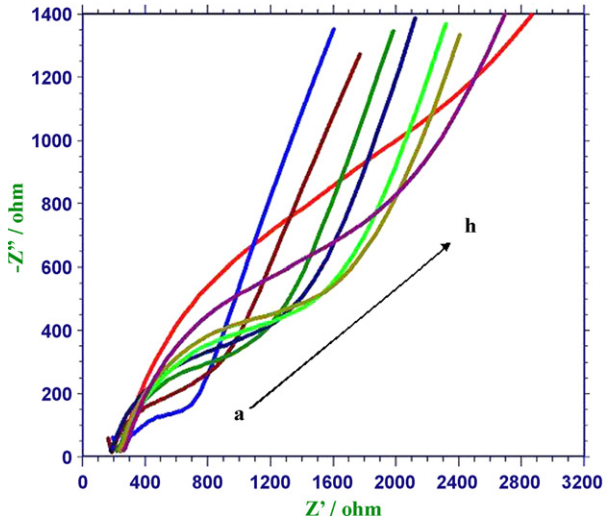

Fig. 5. Nyquist diagrams of 1.0 mmol/L $[Fe(CN)_6]^{3-/4-}$ recorded at (a) ssDNA/Fe_2O_3/SPAN/CILE and after hybridization reaction with different concentrations of PEPCase gene target sequence: (b) 1.0×10^{-13} mol/L, (c) 1.0×10^{-12} mol/L, (d) 1.0×10^{-11} mol/L, (e) 1.0×10^{-10} mol/L, (f) 1.0×10^{-9} mol/L, (g) 1.0×10^{-8} mol/L and (h) 1.0×10^{-7} mol/L.

4. Conclusions

A conductive Fe_2O_3/SPAN membrane was developed on CILE for the simple, rapid, specific electrochemical impedance detection of DNA hybridization. The combination CILE with conductive materials provided a promising functional interface for the immobilization of DNA probe. It was demonstrated that the proposed approach had a wide detection range with a low detection limit. Moreover, the reported biosensor achieved impressive selectivity with successful discrimination of the target DNA from mismatch sequences. This novel DNA sensing architecture may have the potential for the detection of target DNA in complex samples, even clinical analytes, and the simple strategy described here may be facile to apply in DNA damage analysis and diagnostics.

Acknowledgments

This work was supported by the National Natural Science Foundation of China (No. 20635020, 20805025), Foundation of Qingdao City (No. 09-1-3-25-jch) and Doctoral Foundation of the Ministry of Education of China (No. 20060426001).

Appendix A. Supplementary data

Supplementary data associated with this article can be found, in the online version, at doi:10.1016/j.bios.2009.07.032.

References

Ao, L.M., Gao, F., Pan, B.F., He, R., Cui, D.X., 2006. Anal. Chem. 78, 1104–1106.
Chen, J.H., Zhang, J., Wang, K., Lin, X.H., Huang, L.Y., Chen, G.N., 2008. Anal. Chem. 80, 8028–8034.
Cheng, F.Y., Su, C.H., Yang, Y.S., Yeh, C.S., Tsai, C.Y., Wu, C.L., Wu, M.T., Shieh, D.B., 2005. Biomaterials 26, 729–738.
Cheng, Y.X., Liu, Y.J., Huang, J.J., Li, K., Xian, Y.Z., Zhang, W., Jin, L.T., 2009. Electrochim. Acta 54, 2588–2594.
Feng, K.J., Yang, Y.H., Wang, Z.J., Jiang, J.H., Shen, G.L., Yu, R.Q., 2006. Talanta 70, 561–565.
Franzoi, A.C., Dupont, J., Spinelli, A., Vieira, I.C., 2009. Talanta 77, 1322–1327.
Gao, F.X., Yuan, R., Chai, Y.Q., Chen, S.H., Cao, S.R., Tang, M.Y., 2007. J. Biochem. Biophys. Methods 70, 407–413.
Gorodetsky, A.A., Ebrahim, A., Barton, J.K., 2008. J. Am. Chem. Soc. 130, 2924–2925.
Kukol, A., Li, P., Estrela, P., Ferrigno, P.K., Migliorato, P., 2008. Anal. Biochem. 374, 143–153.
Li, F., Chen, W., Zhang, S.S., 2008. Biosens. Bioelectron. 24, 787–792.
Maleki, N., Safavi, A., Farjami, E., Tajabadi, F., 2008. Anal. Chim. Acta 611, 151–155.
Maleki, N., Safavi, A., Tajabadi, F., 2006. Anal. Chem. 78, 3820–3826.
Musameh, M.M., Kachoosangi, R.T., Compton, R.G., 2008. Analyst 133, 133–138.
Park, J.Y., Kwon, S.H., Park, J.W., Park, S.M., 2008. Anal. Chim. Acta 619, 37–42.
Prabhakar, N., Arora, K., Singh, H., Malhotra, B.D., 2008. J. Phys. Chem. B 112, 4808–4816.

Qu, S., Huang, F., Chen, G., Yu, S.N., Kong, J.L., 2007. Electrochem. Commun. 9, 2812–2816.
Radeva, T., Petkanchin, I., 1997. J. Colloid Interface Sci. 196, 87–91.
Shangguan, X.D., Zhang, H.F., Zheng, J.B., 2008. Electrochem. Commun. 10, 1140–1143.
Sonti, S.V., Bose, A., 1995. J. Colloid Interface Sci. 170, 575–585.
Sun, W., Gao, R.F., Jiao, K., 2007. J. Phys. Chem. B 111, 4560–4567.
Sun, W., Li, Y.Z., Duan, Y.Y., Jiao, K., 2008. Biosens. Bioelectron. 24, 994–999.
Tang, D.P., Yuan, R., Chai, Y.Q., 2008. Anal. Chem. 80, 1582–1588.
Teles, F.R.R., Fonseca, L.P., 2008. Talanta 77, 606–623.
Wang, D.B., Song, C.X., Zhao, Y.H., Yang, M.L., 2008. J. Phys. Chem. C 112, 12710–12715.
Wang, S.F., Tan, Y.M., Zhao, D.M., Liu, G.D., 2008. Biosens. Bioelectron. 23, 1781–1787.
Welton, T., 1999. Chem. Rev. 99, 2071–2083.
Xiao, F., Zhao, F.Q., Li, J.W., Liu, L.Q., Zeng, B.Z., 2008. Electrochim. Acta 53, 7781–7788.
Yang, J., Jiao, K., Yang, T., 2007. Anal. Bioanal. Chem. 389, 913–921.
Yang, Y.H., Wang, Z.J., Yang, M.H., Li, J.S., Zheng, F., Shen, G.L., Yu, R.Q., 2007. Anal. Chim. Acta 584, 268–274.
Yang, T., Zhou, N., Zhang, Y.C., Zhang, W., Jiao, K., Li, G.C., 2009. Biosens. Bioelectron. 24, 2165–2170.
Zhang, W., Yang, T., Huang, D.M., Jiao, K., Li, G.C., 2008a. J. Membr. Sci. 325, 245–251.
Zhang, W., Yang, T., Jiang, C., Jiao, K., 2008b. Appl. Surf. Sci. 254, 4750–4756.
Zhang, C.Q., Li, G.C., Peng, H.R., 2009. Mater. Lett. 63, 592–594.
Zhang, W., Yang, T., Zhuang, X.M., Guo, Z.Y., Jiao, K., 2009. Biosens. Bioelectron. 24, 2417–2422.
Zhang, Y.L., Wang, Y., Wang, H.B., Jiang, J.H., Shen, G.L., Yu, R.Q., Li, J.H., 2009. Anal. Chem. 81, 1982–1987.
Zhu, N.N., Zhang, A.P., Wang, Q.J., He, P.G., Fang, Y.Z., 2004. Anal. Chim. Acta 510, 163–168.
Zhuo, Y., Yuan, P.X., Yuan, R., Chai, Y.Q., Hong, C.L., 2009. Biomaterials 30, 2284–2290.